Uzbek Journal "Problems of Mechanics"

Research Article

DOI: 10.68846/pmjournal-2026-37-00011

Mathematical modelling of pollutant dispersion in the atmosphere with allowance for the spatial–temporal variation of temperature

I.S. Nabiyeva[1*], **O.S. Juraboyeva**[2], **G. B. Samanova**[3]

[1] Kimyo International University in Tashkent Branch Samarkand, Digital Technologies and Artificial Intelligence Development Research Institute

[2] Digital Technologies and Artificial Intelligence Development Research Institute, 17A Buz-2, Tashkent, 100125, Uzbekistan

[3] Tashkent State Medical University, 2 Farobiy Street, Tashkent, 100109, Uzbekistan

[*] **Corresponding author:** irodamubina777@gmail.com

Received: 04 Jule 2026 | **Revised:** 15 August 2026 | **Accepted:** 05 September 2026 | **Published:** 30 September 2026

ABSTRACT

A three-dimensional model is developed for the dispersion of harmful substances in the atmospheric surface layer with allowance for the spatial–temporal variation of temperature. The advection–diffusion equation for the pollutant, written in conservative form with a temperature-dependent gravitational-settling flux, is solved together with a temperature (energy) equation; the dynamic viscosity (Sutherland's law), the air density, the molecular diffusivity and the settling velocity are functions of the local temperature, and the atmospheric thermal stability enters the vertical turbulent diffusion through the gradient Richardson number and a monotone stability function. The problem is discretised by an explicit finite-volume scheme with upwind advection and a combined Courant–Friedrichs–Lewy step, point sources are prescribed as grid-independent mass rates, and the ground boundary is treated as dry deposition with a tracked deposited mass. The scheme is validated against an analytical Gaussian solution and verified by machine-precision mass conservation and grid/time convergence. Two reproducible regimes are computed: a daytime unstable case ($Ri < 0$) and a night-time surface inversion ($Ri > 0$). Under the inversion the vertical mixing is suppressed by more than an order of magnitude, the pollutant is confined to a shallow near-surface layer with an in-layer peak about three times the daytime value, and only about 18% of the emitted mass is ventilated out of the region against about 70% in the daytime. The example is illustrative rather than a site-specific prediction.

KEYWORDS

advection-diffusion equation, temperature inversion, thermal stability, Richardson number, gravitational settling, finite-volume method, mass conservation.

1. Introduction

The transport of fine particulate matter (PM2.5, PM10) and gaseous pollutants over the atmospheric surface layer is a pressing environmental problem, and its quantitative prediction requires models that reproduce the governing physical processes. Among these, temperature plays a special role: it controls the molecular and turbulent diffusion, the air density and viscosity, the gravitational settling velocity of particles, and, above all, the vertical thermal stability of the atmosphere [1]. During the day the heating of the ground generates convective mixing; at night a surface temperature inversion suppresses vertical exchange and can confine pollutants to a shallow layer near the ground. The dispersion process therefore cannot be predicted accurately without allowance for the spatial–temporal variation of temperature.

The Eulerian, Gaussian and Lagrangian approaches are most widely used in atmospheric-pollution modelling [2–5]. Operational Eulerian systems such as CMAQ compute advection, diffusion, emission and deposition together on a three-dimensional grid [2, 4]; Gaussian models are simple and fast but assume steady, homogeneous conditions [6–8]; Lagrangian models are flexible for time-varying winds [9]. Micallef and Micallef [6] corrected the Gaussian plume for multiple reflections, and Kafle et al. [7] modelled one-dimensional dispersion from the advection–diffusion equation. Numerical treatments of the transport equation and its optimal parameters [10], and models accounting for surface heterogeneity, vegetation and relief [11, 12], are well developed. In earlier work by the authors [13–18] the dispersion was modelled as a function of the physical–mechanical properties of the particles, the wind and the particle diameter, with the diffusion coefficient computed dynamically; there, however, the temperature was treated mainly as a constant or a single-step parameter, and the vertical stability was not resolved.

The specific new element of the present work is a compact but internally consistent coupling: the concentration equation is written in conservative form and solved together with a temperature field, the temperature-dependent air properties and settling velocity are included, and, in particular, the atmospheric stability is introduced into the vertical diffusion through the Richardson number, so that daytime convection and a night-time inversion can be compared quantitatively within one reproducible, mass-conservative and verified numerical framework. We do not claim that other models ignore temperature altogether; rather, we provide a verified formulation and an explicit day-versus-night comparison. The full nomenclature is given at the end of the paper.

2. Problem statement

Let $C(x, y, z, t)$ be the mass concentration of the pollutant (mass per unit volume of air, mg/m^3). A solute balance over a fixed control volume, with the settling flux written in divergence (conservative) form, gives

$$\frac{\partial C}{\partial t} + \frac{\partial (uC)}{\partial x} + \frac{\partial (vC)}{\partial y} + \frac{\partial \left[(w - w_g(T))C\right]}{\partial z} = \frac{\partial}{\partial x}\left(D_x \frac{\partial C}{\partial x}\right) + \frac{\partial}{\partial y}\left(D_y \frac{\partial C}{\partial y}\right) + \frac{\partial}{\partial z}\left(D_z \frac{\partial C}{\partial z}\right) - \sigma C - k_{veg} C + S_C. \tag{1}$$

where u, v, w are the wind components, $w_g(T)$ the gravitational settling velocity, D_x, D_y, D_z the effective diffusivities, σ the wet-scavenging coefficient, k_{veg} the first-order vegetation-uptake rate (s^{-1}), and S_C the emission source (below). Because the mean flow is taken incompressible, $\partial_x u + \partial_y v + \partial_z w = 0$, the advection may equivalently be written in non-conservative form for u, v, w; the settling contribution, however, is kept in the flux form $\partial_z \left[(w - w_g)\, C\right]$, which for a temperature-dependent $w_g(T)$ retains the term $-C\, \partial_z w_g$ that a non-conservative writing would omit. This is essential for global mass conservation and is respected by the discretisation.

The temperature field is governed by the energy-transport equation

$$\frac{\partial T}{\partial t} + u\frac{\partial T}{\partial x} + v\frac{\partial T}{\partial y} + w\frac{\partial T}{\partial z} = \frac{\partial}{\partial z}\left(\varkappa_z \frac{\partial T}{\partial z}\right) + S_T, \tag{2}$$

with $\varkappa_z$ the thermal diffusivity and S_T the surface heating/cooling. In the present study the meteorology is taken horizontally uniform, so that $T = T(z, t)$; the coupling is one-way, $T \to C$ (the temperature controls the pollutant transport, and the small pollutant loading does not feed back on the temperature). This is stated explicitly and is a deliberate modelling choice.

Temperature-dependent properties. The dynamic viscosity follows Sutherland's law and the density the ideal-gas law,

$$\eta(T) = \eta_0 (\frac{T}{T_0})^{3/2} \frac{T_0 + S_\eta}{T + S_\eta}, \qquad \rho_a(T) = \frac{P}{R_a T}, \tag{3}$$

with $\eta_0 = 1.716 \times 10^{-5}$ Pa·s, $T_0 = 273.15$ K, $S_\eta = 110.4$ K, $R_a = 287$ J/(kg·K). The molecular diffusivity of a particle of diameter d follows the Stokes–Einstein relation, and the settling velocity Stokes' law,

$$D_m(T) = \frac{k_B T}{3\pi\eta(T) d}, \qquad w_g(T) = \frac{\left(\rho_p - \rho_a(T)\right)\, g\, d^2}{18\, \eta(T)}. \tag{4}$$

For the coarse-particle case considered here ($d = 10\ \mu$m) the Stokes regime applies (particle Reynolds number $\ll 1$); for larger particles a drag correction would be required. It should be emphasised that D_m is a molecular property of order 10^{-12} m^2/s and is negligible next to the turbulent diffusivities (see below); it is retained only for completeness [19].

Thermal stability. Using the potential temperature $\theta = T + \left(g/c_p\right) z$, the gradient Richardson number is

$$Ri = \frac{g}{\theta} \frac{\partial \theta / \partial z}{(\partial u/\partial z)^2 + (\partial v/\partial z)^2}. \tag{5}$$

The wind is prescribed by a surface-layer power-law profile $u(z) = u_r\, (z/z_r)^p$, $v(z) = v_r\, (z/z_r)^p$ (so the shear $\partial_z u, \partial_z v$ is non-zero and Ri is well defined); the denominator is bounded below by the mechanical surface-layer shear $u_*/(\varkappa z)$ to keep Ri finite, and Ri is limited to the operational range $[-2, 2]$. The vertical turbulent diffusivity is modulated by a *monotone* stability function,

$$D_z(z) = D_{z0}\, f(Ri), \qquad f(Ri) = \begin{cases} (1 - 16\, Ri)^{1/2}, & Ri < 0 \text{ (unstable)}, \\ (1 + 5\, Ri)^{-2}, & Ri \geqslant 0 \text{ (stable)}, \end{cases} \tag{6}$$

clipped to $f \in \left[10^{-3}, 5\right]$. For $Ri \geqslant 0$ this form decreases monotonically toward a small residual as the stratification strengthens, so that it suppresses mixing throughout the stable range without the spurious re-growth of the earlier expression $(1 - 5Ri)^2$ (which increases again for $Ri > 0.2$); the small floor represents residual sporadic mixing and keeps $D_z > 0$. The vegetation uptake is a first-order linear sink, $k_{veg} C$ with $k_{veg} = \gamma_{veg} \beta_{veg}$ (s^{-1}); an explicit update requires $k_{veg} \Delta t < 1$, which is satisfied and preserves non-negativity.

Source term. Each point source is prescribed by its *mass emission rate* E_s (mg/s) and normalised over the cell volume,

$$S_C\,(\mathbf{r}, t) = \sum_s \frac{E_s}{\Delta x\, \Delta y\, \Delta z}\, \mathbf{1}_{\{\mathbf{r} = \mathbf{r}_s\}}, \tag{7}$$

so that the integral emission $\int S_C\, dV = \sum_s E_s$ is independent of the mesh; refining the grid keeps the total emission fixed (the nodal peak, which represents a point-source singularity, is inherently grid-dependent and is not used as a convergence metric).

Initial and boundary conditions. Initially $C = 0$ and $T = T_0(z)$. On the lateral boundaries a zero inflow is imposed on the upwind faces and a zero-gradient outflow elsewhere; the top is zero-gradient. On the ground a *dry-deposition* condition is used,

$$\left(D_z \frac{\partial C}{\partial z}\right)|_{z=0} = v_d C|_{z=0}, \qquad \frac{dm_{dep}}{dt} = v_d C|_{z=0}, \tag{8}$$

with deposition velocity v_d; the mass removed from the air is accumulated as the surface deposit m_{dep}, so that deposition is a genuine loss from the air and not merely a reflecting (zero-flux) wall. The two conditions — reflection and deposition — are thus clearly distinguished, and the reported deposited mass closes the budget.

3. Numerical method

The domain is covered by a uniform grid $x_i = i\Delta x$, $y_j = j\Delta y$, $z_k = k\Delta z$, and time by $t^n = n\Delta t$. Equation (1) is discretised by a conservative finite-volume scheme: the advective (including settling) fluxes are evaluated at cell faces by first-order upwinding, and the diffusive fluxes by central face differences with interface diffusivities $D_{k\pm1/2} = \frac{1}{2}\,(D_k + D_{k\pm1})$, so that what leaves one cell enters the next and the scheme

conserves mass exactly. The temperature (2) is advanced first at each step, the temperature-dependent parameters η, ρ_a, D_m, w_g and the stability-corrected $D_z(z)$ are recomputed, and the concentration is then advanced explicitly.

Because the advection and diffusion act simultaneously, the explicit step must satisfy a *combined* stability condition rather than the minimum of the separate advective and diffusive limits (the latter can give a negative central coefficient even when each separate limit holds). The admissible step used here is

$$\Delta t \leqslant \frac{\nu}{\frac{|u|_{\max}}{\Delta x} + \frac{|v|_{\max}}{\Delta y} + \frac{|w - w_g|_{\max}}{\Delta z} + 2\left(\frac{D_x}{\Delta x^2} + \frac{D_y}{\Delta y^2} + \frac{D_{z,max}}{\Delta z^2}\right) + \sigma + k_{veg}}, \quad \nu < 1, \tag{9}$$

which guarantees non-negative update coefficients for the full advection–diffusion–sink stencil; the same bound is applied to the temperature step. Since $D_z(z)$ depends on the stability, Δt is evaluated from the largest local diffusivity.

4. Computational experiments and results

The domain was 8×6 km horizontally and 600 m high, resolved by $81 \times 61 \times 61$ nodes ($\Delta x = \Delta y = 100$ m, $\Delta z = 10$ m). Three low-level sources (representative of near-ground urban emissions) were placed at $x = 2$ km, $y = 3, 4, 5$ km, at height 20 m, each with an emission rate $E_s = 5 \times 10^3$ mg/s; the particle type was dust ($d = 10$ μm, $\rho_p = 2000$ kg/m^3), giving a settling velocity $w_g \approx 0.60$ cm/s and a deposition velocity $v_d \approx 0.60$ cm/s. The reference wind was $u_r = 3.0$, $v_r = 1.5$ m/s at $z_r = 10$ m ($p = 0.2$), and the base diffusivities $D_x = 30$, $D_y = 20$, $D_{z0} = 8$ m^2/s. Two regimes were computed to $t = 3600$ s: a *daytime* case (surface heated, unstable) and a *night* case (surface cooled by up to 12 K, forming a ground-based inversion). In the lowest 400 m (the layer shown in the figures) the computed Richardson number lies in $Ri \in [-2, -0.05]$ (day) and $Ri \in [0.06, 2]$ (night); the corresponding D_z ranges from about 11–40 m^2/s (day, enhanced) down to 0.07–4.6 m^2/s (night, suppressed). Thus, unlike the earlier draft, the inversion regime ($Ri > 0$) is actually computed, not merely tabulated.

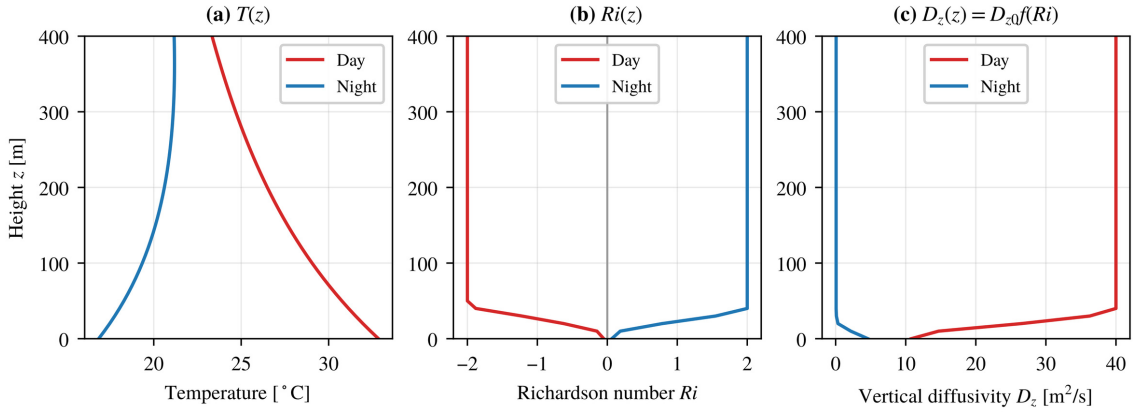


Figure 1. Vertical profiles for the daytime and night regimes: (a) temperature $T(z)$; (b) gradient Richardson number $Ri(z)$; (c) stability-corrected vertical diffusivity $D_z(z) = D_{z0} f(Ri)$. The night inversion gives $Ri > 0$ and an order-of-magnitude suppression of D_z.

Figure 1 shows the temperature, Richardson-number and vertical-diffusivity profiles. In the daytime the near-surface air is superadiabatic ($Ri < 0$) and D_z is enhanced; at night the surface-based inversion gives $Ri > 0$ and suppresses D_z by more than an order of magnitude, which is the mechanism of near-surface trapping.

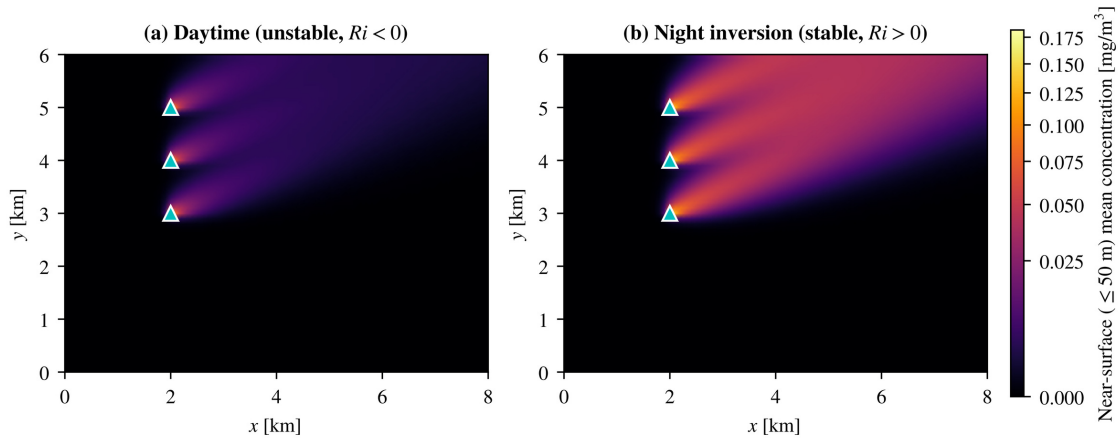


Figure 2. Near-surface ($\leqslant$ 50 m) mean concentration at $t = 3600$ s: (a) daytime and (b) night inversion. Triangles mark the three near-ground sources ($x = 2$ km, $y = 3, 4, 5$ km). Flow is toward the east–north-east. The colour scale is square-root stretched to show the dilute part of the plume.

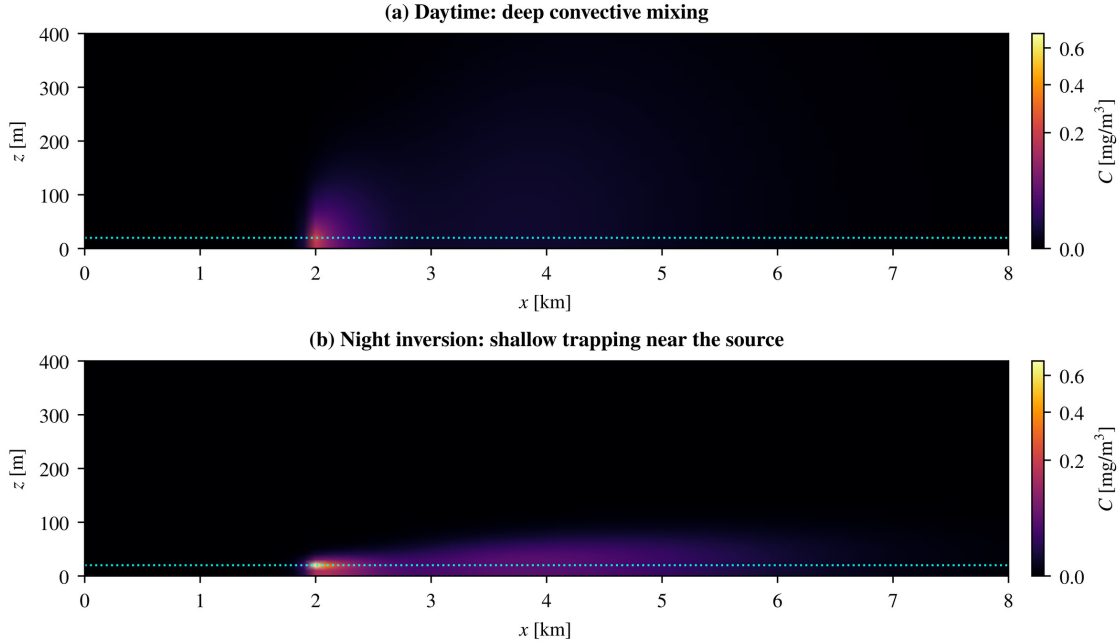


Figure 3. Vertical cross-section of the concentration through the central source ($y = 4$ km): (a) daytime deep convective mixing; (b) night-time shallow trapping near the source height (dotted line at 20 m). Note the confinement of the plume to a thin layer at night. The colour scale is square-root stretched.

The horizontal near-surface fields (Fig. 2) and the vertical cross-sections (Fig. 3) show the physical contrast directly: in the daytime the plume is mixed through a deep layer and diluted, whereas at night it is confined to a shallow layer near the source and reaches higher concentrations there. Quantitatively, the peak concentration in the source layer is about three times larger at night than in the daytime, while the near-surface horizontal footprint is more compact.

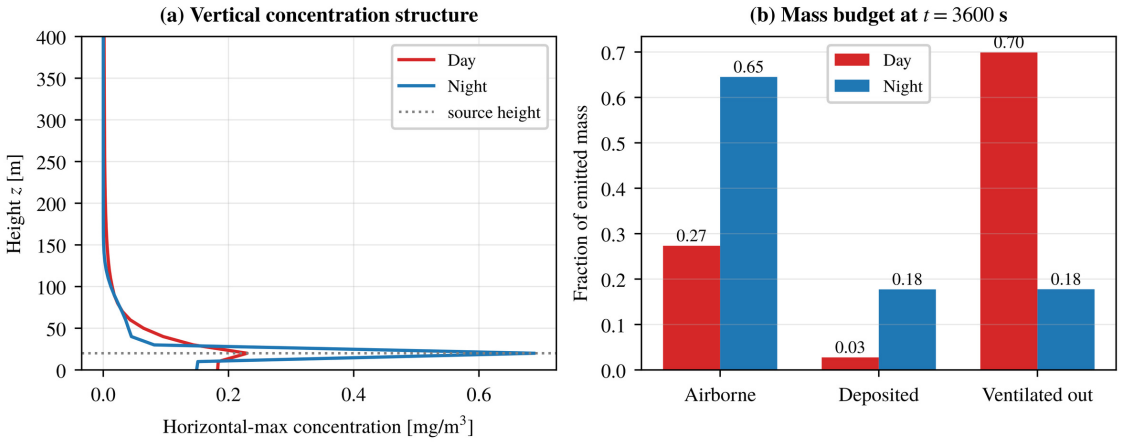


Figure 4. Day versus night: (a) vertical profile of the horizontal-maximum concentration (the night profile is confined near the source height, the daytime profile is spread through depth); (b) mass budget at $t = 3600$ s as fractions of the emitted mass (airborne, deposited, ventilated out of the domain).

The most robust, grid-independent measure of the effect is the mass budget (Fig. 4b). In the daytime about 70% of the emitted mass is ventilated out of the region and only 27% remains airborne within it; at night the ventilation drops to about 18%, while 65% remains airborne locally and 18% is deposited. In other words, the inversion retains the pollutant in the source region instead of dispersing it, which is the quantitative content of the "trapping" effect. We emphasise that the *absolute* peak concentration near a point source is grid-dependent (a point-source singularity), whereas the mass-budget fractions and the day/night ratio are grid-robust (Section 5); the conclusions are therefore drawn from the latter.

Temperature effect on molecular diffusion. From (4), raising the temperature from 298 to 308 K increases D_m by only about 0.77% (from 2.38×10^{-12} to 2.39×10^{-12} m^2/s); this is a correction of the earlier 3–4% estimate. Since $D_m \sim 10^{-12}$ m^2/s is about twelve orders of magnitude smaller than the turbulent diffusivities (8–40 m^2/s), molecular diffusion cannot account for the observed horizontal spreading, which is turbulent. The genuine temperature effects are those on the stability (dominant) and, weakly, on the settling velocity through $\eta(T)$ and $\rho_a(T)$.

5. Verification and validation

The numerical scheme was verified and validated before drawing physical conclusions. *Analytical validation.* For constant coefficients and pure diffusion, the computed spreading of a Gaussian puff was compared with the exact solution $C = \frac{M}{4\pi Dt}\exp\left(-r^2/4Dt\right)$; the L_2 error decreases from 0.79% at $h = 67$ m to 0.19% at $h = 33$ m, i.e. second-order convergence (Fig. 5a). *Mass conservation.* In a closed domain with reflecting boundaries and a source but no deposition or sink, the emitted mass equals the airborne mass to machine precision, $|M_{in} - M_{air}|\,/M_{in} \approx 1 \times 10^{-14}$, confirming that the finite-volume discretisation is exactly conservative. *Grid convergence.* For the night case the mass-budget fractions change by less than 1% under refinement from $N_x = 61$ to 121 (Fig. 5b), and the day/night source-layer peak ratio is 3.2 and 3.0 on the two coarser and finer grids — i.e. the physical contrast is grid-robust. *Time-step convergence.* Halving Δt (via $\nu = 0.6, 0.4, 0.2$) leaves the near-surface concentration unchanged to three significant figures.

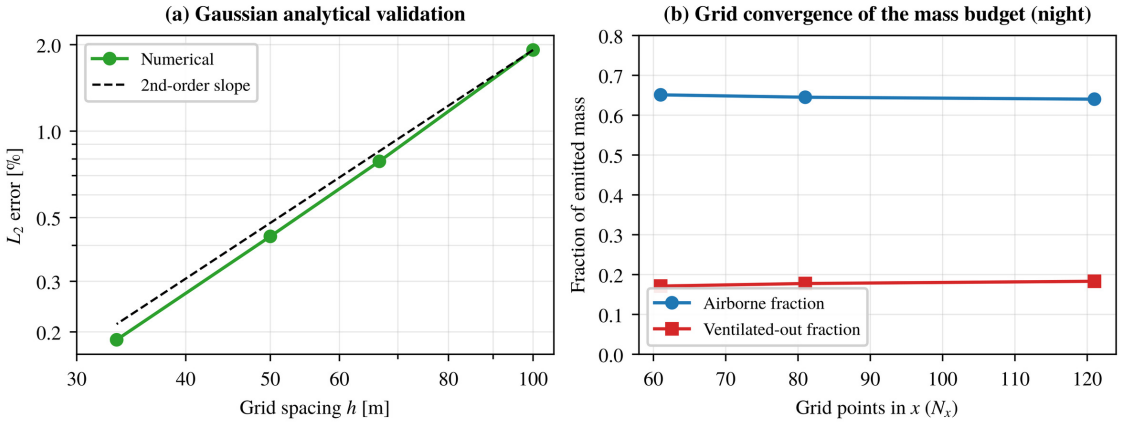


Figure 5. Verification: (a) L_2 error of the computed Gaussian spreading against the analytical solution versus grid spacing (second-order slope shown); (b) grid convergence of the night mass-budget fractions (airborne and ventilated-out).

6. Concluding remarks

A three-dimensional, mass-conservative and verified model has been developed for the dispersion of pollutants in the atmospheric surface layer with allowance for the spatial–temporal variation of temperature. The pollutant equation is written in conservative form with a temperature-dependent settling flux and is coupled one-way to a temperature field; the air properties and settling velocity depend on the local temperature, and the thermal stability enters the vertical diffusion through the Richardson number and a monotone stability function. The explicit finite-volume scheme uses a combined CFL step, prescribes sources as grid-independent mass rates, and treats the ground as a depositing surface. The scheme was validated against an analytical Gaussian solution and verified by machine-precision mass conservation and grid/time convergence. Two reproducible regimes were computed: under the night-time surface inversion the vertical mixing is suppressed by more than an order of magnitude, the pollutant is confined to a shallow near-surface layer with an in-layer peak about three times the daytime value, and the local retention rises sharply (only ~ 18% of the mass ventilated out, against ~ 70% in the daytime). The computation is an illustrative model case, not a site-specific prediction; quantitative environmental forecasting would require measured emissions and meteorology. Natural extensions include two-way thermal coupling, spatially variable meteorology, multi-component chemistry, and validation against field measurements.

Declarations

Author Contributions: Conceptualization, I.S.N.; methodology, I.S.N.; software, I.S.N.; validation, O.S.J.; visualization, O.S.J.; writing—original draft preparation, I.S.N.; writing—review and editing, O.S.J. All authors have read and agreed to the published version of the manuscript. The specific contributions of G.B.S. were not specified in the submitted source and require author confirmation.

Funding: This research received no specific grant from any funding agency in the public, commercial, or not-for-profit sectors.

Ethics Approval: Not applicable. This is a mathematical and numerical study involving no human or animal subjects.

Informed Consent and Consent for Publication: Not applicable. The submitted mathematical study includes no human participants or identifiable participant data.

Data Availability Statement: The finite-volume solver and the data underlying the figures, the verification tests and the mass budgets are available from the corresponding author on reasonable request.

Acknowledgments: The submitted manuscript does not specify acknowledgments. The authors should confirm whether any acknowledgments are required before publication.

Conflicts of Interest: The authors declare no conflict of interest.

Artificial Intelligence Disclosure: An AI assistant was used to prepare the English journal-template LaTeX formatting of this manuscript. The authors must confirm any further AI use and review this disclosure prior to publication.

Nomenclature and Abbreviations

Symbol / acronym	Definition
C	pollutant mass concentration (mg/m^3)
d	particle diameter
T	temperature (K)
σ	scavenging rate
θ	potential temperature
k_{veg}	vegetation-uptake rate (s^{-1})
u, v, w	wind components (m/s)
E_s	source mass rate (mg/s)
w_g	settling velocity
S_C, S_T	concentration and heat sources
v_d	deposition velocity
Ri	gradient Richardson number
D_x, D_y, D_z	turbulent diffusivities (m^2/s)
$f(Ri)$	stability function
D_{z0}	base vertical diffusivity
u_*	friction velocity
D_m	molecular diffusivity
$\varkappa$	von Kármán constant
$\varkappa_z$	thermal diffusivity
m_{dep}	deposited mass
η	dynamic viscosity
$\Delta x, \Delta y, \Delta z, \Delta t$	grid steps
ρ_a, ρ_p	air and particle density

References

[1] Stull RB. An Introduction to Boundary Layer Meteorology. Kluwer Academic; 1988.

[2] Byun D, Schere KL. Review of the governing equations, computational algorithms, and other components of the Models-3 Community Multiscale Air Quality (CMAQ) modeling system. Appl Mech Rev. 2006;59:51–77. https://doi.org/10.1115/1.2128636.
[3] Jacobson MZ. Fundamentals of Atmospheric Modeling. 2nd ed. Cambridge University Press; 2005.
[4] Zhang Y. Online-coupled meteorology and chemistry models: history, current status, and outlook. Atmos Chem Phys. 2008;8:2895–2932. https://doi.org/10.5194/acp-8-2895-2008.
[5] Holmes NS, Morawska L. A review of dispersion modelling and its application to the dispersion of particles. Atmos Environ. 2006;40:5902–5928. https://doi.org/10.1016/j.atmosenv.2006.06.003.
[6] Micallef A, Micallef C. The Gaussian plume model equation for atmospheric dispersion corrected for multiple reflections. Sci. 2024;6(3):49. https://doi.org/10.3390/sci6030049.
[7] Kafle J, Adhikari K, Poudel E. Air pollutant dispersion using advection-diffusion equation. Nepal J Environ Sci. 2024;12(1):1–6.
[8] Turner DB. Workbook of Atmospheric Dispersion Estimates: An Introduction to Dispersion Modeling. 2nd ed. CRC Press; 1994.
[9] Wyngaard JC. Turbulent dispersion modeling in the boundary layer. J Atmos Sci. 1982;39(6):1342–1353.
[10] Jejeniwa O, Gidey H, Appadu A. Numerical modeling of pollutant transport: results and optimal parameters. Symmetry. 2022;14:2616. https://doi.org/10.3390/sym14122616.
[11] Ravshanov N, Nazarov S, Nazarov E, Boborahimov B. Development of a mathematical model of aerosol particles' distribution process in the surface layer of the atmosphere taking into account the Earth's heterogeneous surface. AIP Conf Proc. 2024;3004:060004.
[12] Ravshanov N, Nazarov SE, Boborahimov B. Modeling the process of pollutant spread in the atmosphere with account for the capture of particles by vegetation elements. Lobachevskii J Math. 2024;45(3):1213–1226.
[13] Nabieva IS. Numerical modeling of the transport and diffusion of pollutant particles taking into account airflow characteristics and temperature. Probl Comput Appl Math. 2025;1(63):27–40.
[14] Ravshanov N, Nabieva IS. Mathematical modeling of the process of harmful substances dispersion in the atmosphere taking into account temperature and physical–chemical properties. Int J Theor Appl Issues Digit Technol. 2024;7(4):27–32.
[15] Ravshanov N, Nabieva I, Sapaeva D, Hojiev N. Mathematical modeling of the distribution of pollutants in the atmosphere, taking into account their physical and mechanical properties. Proc SPIE. 2025;13662:136620K. https://doi.org/10.1117/12.3072577.
[16] Ravshanov N, Nabieva IS, Boborakhimov BI. Software for predicting the spread of harmful substances in the atmosphere, taking into account their type and wind speed. Probl Comput Appl Math. 2025;2/2(66):54–59.
[17] Boborakhimov B, Nabiyeva I, Tashtemirova N, Juraboyeva O. Mathematical modeling of the dispersion of pollutants in the atmosphere, taking into account their physico-mechanical properties and hygroscopic parameters. AIP Conf Proc. In press.
[18] Ravshanov N, Boborakhimov B, Nabiyeva I. Mathematical modeling of the distribution of harmful substances in the atmosphere in variable-direction currents. E3S Web Conf. In press.
[19] Seinfeld JH, Pandis SN. Atmospheric Chemistry and Physics: From Air Pollution to Climate Change. 3rd ed. John Wiley & Sons; 2016.

Disclaimer of Liability/Publisher's Note

The statements, opinions, and data contained in all publications are solely those of the individual author(s) and contributor(s) and do not necessarily reflect the views of the Publisher, the Journal, or the editors. The Publisher, the Journal, and the editors disclaim responsibility for any injury to persons or damage to property resulting from any ideas, methods, instructions, or products referred to in the content.